PROPAGATION OF SHOCK WAVES IN A POLYTROPE WITH A TOROIDAL MAGNETIC FIELD

II.* SOLUTION OF COMPLETE DIFFERENTIAL EQUATIONS

By N. K. SINHA†

[*Manuscript received May 2, 1969*]

Summary

The differential equations for the shock parameters along shock rays in the case of propagation of a spherically developed shock wave in a polytrope with a toroidal magnetic field, obtained in Part I, have been integrated numerically for a particular set of initial values. The results are compared with the corresponding results in Part I obtained by neglecting certain small terms and it is found that the effect of this omission is not significant. This substantiates the results and justifies the simplification made in Part I.

I. INTRODUCTION

The terms neglected in the differential equations (16) obtained for the shock parameters along shock rays in Part I, though small compared with the remaining terms, involve unknown spatial derivatives of the velocity components. Therefore, a method to determine these derivatives at unknown points is required so that the differential equations including these terms can be integrated. In the present paper, Butler's (1960) method of dealing with such terms has been extended and the relevant set of differential equations including these terms has been integrated for a particular set of initial values. A comparison of the results obtained with the corresponding results of Part I helps to ascertain the error involved as a result of the omission of these terms.

There are available an infinite number of bicharacteristics, the curves of contact of the characteristic surfaces with the characteristic conoid, through each point on the solution surface for a system of quasi-linear hyperbolic partial differential equations in three independent variables (Courant and Hilbert 1965). From the point of view of wave propagation, these bicharacteristics define the directions along which disturbances are propagated. The compatibility relations, which involve terms containing the spatial derivatives of the velocity components along some of the bicharacteristics, are invoked to obtain further equations containing these derivatives. In the present case, however, it is found that two of the four spatial derivatives always appear, combined only as their sum, both in the differential equations as well as in the bicharacteristic relations, leaving only three unknown terms. Thus we require compatibility relations only along three bicharacteristics for the evaluation of these

* Part I, *Aust. J. Phys.*, 1969, **22**, 589–603.

† Department of Mathematics, Monash University, Clayton, Vic. 3168; present address: Department of Mathematics, Regional Institute of Technology, Jamshedpur, India.

terms at a point. The datum region at an initial time $t_0-\Delta t$ is the field of flow bounded by the shock front at time $t_0-\Delta t$. This restricts the domain of dependence of a point P^* (with $t^* > t_0-\Delta t$; Fig. 1) and, therefore, we have to consider only those bicharacteristics of the retrograde characteristic conoid with vertex at P^* which meet the datum region at real points. Three such bicharacteristics (Butler 1960) are chosen and difference relations are employed along them to elicit equations for the determination of the three unknown terms.

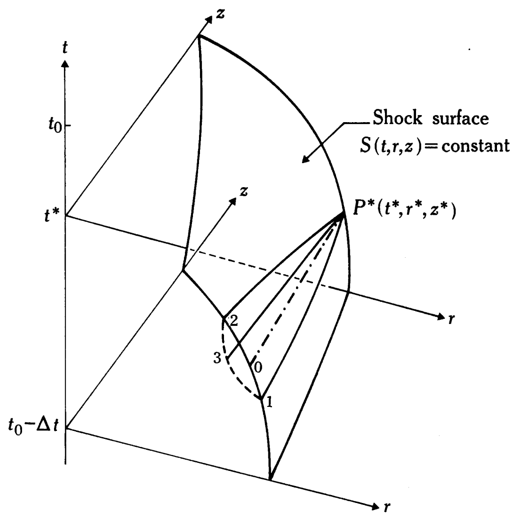

Fig. 1.—Diagram illustrating the segment of the shock ray (chained contour) and the bicharacteristic segments 1, 2, and 3 through a point P^* on the shock.

A step-by-step numerical integration scheme is set up at different points on the initial shock front to determine their positions after a time Δt and to determine the corresponding values of the shock parameters. The process is repeated to find the subsequent positions and orientations of the front. With the knowledge of these quantities, the flow immediately behind the front can be determined with the help of shock relations.

II. Compatibility Relations

The characteristic surface elements $\mathrm{d}h(r,z,t) = 0$ through any point for the set of equations (I1) (equations (1) of Part I) satisfy the equation

$$\left(\frac{\mathrm{D}h}{\mathrm{D}t}\right)^3\left[\left(\frac{\mathrm{D}h}{\mathrm{D}t}\right)^2-\left(b^2+c^2\right)\left\{\left(\frac{\partial h}{\partial r}\right)^2+\left(\frac{\partial h}{\partial z}\right)^2\right\}\right] = 0,$$

and represent the possible manifolds of discontinuity or wave fronts associated with the motion of the fluid (Courant and Hilbert 1965). We use the same notations as in Part I. The characteristic satisfying $\mathrm{D}h/\mathrm{D}t = 0$ represents a streamline of the flow, whereas the second factor in square brackets represents the local normal cone, and the corresponding characteristic surface elements envelope the conoid

$$(\mathrm{d}r-u\,\mathrm{d}t)^2+(\mathrm{d}z-v\,\mathrm{d}t)^2 = A^2\,\mathrm{d}t^2\,.$$

The bicharacteristics through any point can now be expressed parametrically as

$$\mathrm{d}r = (u+A\cos\theta)\mathrm{d}t, \tag{1a}$$

$$\mathrm{d}z = (v+A\sin\theta)\mathrm{d}t, \tag{1b}$$

where $0 \leqslant \theta < 2\pi$, and they represent the propagation velocities of the wave fronts through that point. Let

$$\frac{\mathrm{d}}{\mathrm{d}t} \equiv \frac{\partial}{\partial t}+(u+A\cos\theta)\frac{\partial}{\partial r}+(v+A\sin\theta)\frac{\partial}{\partial z},$$

then $\mathrm{d}/\mathrm{d}t$ denotes differentiation along a bicharacteristic. Using this notation, the basic equations (I1) can be combined to give

$$\begin{aligned}\frac{\mathrm{d}P}{\mathrm{d}t}&+\rho A\cos\theta\frac{\mathrm{d}u}{\mathrm{d}t}+\rho A\sin\theta\frac{\mathrm{d}v}{\mathrm{d}t}\\ &= -\rho A^2\left\{\sin^2\theta\frac{\partial u}{\partial r}-\sin\theta\cos\theta\left(\frac{\partial u}{\partial z}+\frac{\partial v}{\partial r}\right)+\cos^2\theta\frac{\partial v}{\partial z}\right\}\\ &\quad+\frac{\rho A}{\rho_0}\left(\cos\theta\frac{\partial P_0}{\partial r}+\sin\theta\frac{\partial P_0}{\partial z}\right)+\rho A\left(b_0^2-b^2\right)\frac{\cos\theta}{r}-\rho a^2\frac{u}{r},\end{aligned} \tag{2}$$

where the relation

$$\cos\theta\frac{\partial\Phi}{\partial r}+\sin\theta\frac{\partial\Phi}{\partial z} = -\left(\frac{\cos\theta}{\rho_0}\frac{\partial P_0}{\partial r}+\frac{\sin\theta}{\rho_0}\frac{\partial P_0}{\partial z}+\frac{\cos\theta}{r}b_0^2\right),$$

obtained from the equilibrium conditions, has been used. Equation (2) is the compatibility relation, a combination of the basic equations which does not contain any differentiation in the direction normal to the characteristic surface, along the bicharacteristic curve specified by θ.

III. Determination of $\dfrac{\partial u}{\partial r}$, $\dfrac{\partial u}{\partial z}+\dfrac{\partial v}{\partial r}$, and $\dfrac{\partial v}{\partial z}$ at an Unknown Point

The numerical integration of equations (I16) essentially requires the setting up of a numerical scheme which will enable us to find the solution at time $t = t_0$, if the solution is known at time $t = t_0-\Delta t$. As indicated above, this method suffers from the lack of knowledge of the terms

$$\frac{\partial u}{\partial r}, \qquad \frac{\partial u}{\partial z}+\frac{\partial v}{\partial r}, \qquad \text{and} \qquad \frac{\partial v}{\partial z}$$

involved in equations (I16) at a point $P^*(t^*, r^*, z^*)$, where $t^* > t_0-\Delta t$. To resolve this difficulty, we take three bicharacteristics, given by equations (1) for three different values of θ, through the point P^* (Fig. 1) in the backward direction and apply equation (2) along them in difference form between the point P^* and their points of intersection with the plane $t = t_0-\Delta t$. The three bicharactertistics that we choose correspond to $\theta = \omega^*\pm\chi^*$ and ω^* through the point P^*. The asterisk superscript denotes the value of a variable at the point P^*. The first two of these three bicharacteristics lie on the shock surface. This fact can be shown as follows.

The shock surface $S(t, r, z) =$ constant is spanned by the integral curves of

$$\frac{\mathrm{d}r}{U\cos\omega} = \frac{\mathrm{d}z}{U\sin\omega} = \mathrm{d}t,$$

emanating from the initial shock front. Therefore, at any point $P(t, r, z)$ on the shock surface, we have

$$U\cos\omega\frac{\partial S}{\partial r} + U\sin\omega\frac{\partial S}{\partial z} + \frac{\partial S}{\partial t} = 0. \tag{3a}$$

If a bicharacteristic direction, given by

$$\frac{\mathrm{d}r}{u+A\cos\theta} = \frac{\mathrm{d}z}{v+A\sin\theta} = \mathrm{d}t,$$

through the point P also lies on the surface we have further

$$\left(V\cos\omega + A\cos\theta\right)\frac{\partial S}{\partial r} + \left(V\sin\omega + A\sin\theta\right)\frac{\partial S}{\partial z} + \frac{\partial S}{\partial t} = 0, \tag{3b}$$

with the help of equations (I9). Now using the relation

$$U = -\frac{\partial S}{\partial t}\left\{\left(\frac{\partial S}{\partial r}\right)^2 + \left(\frac{\partial S}{\partial z}\right)^2\right\}^{-\frac{1}{2}}$$

for the shock velocity, we can eliminate the derivatives of S from equations (3) and get $\theta = \omega \pm \chi$ specifying the bicharacteristics through the point P which lie on the surface.

IV. Numerical Integration

General details of the procedure followed in this section remain the same as in Section VI of Part I. A polytrope with the same physical properties has been considered. We take 10 different points on the initial front and numerically integrate the equations (I16), supplemented by equations (I17) and (I18), in conjunction with equations (I6)–(I8) for each of the initial points. The process is iterated and the solution obtained at any subsequent time. For the purpose of integration, however, a second-order Runge–Kutta method has been used which gives, for the system of differential equations

$$\mathrm{d}x_i/\mathrm{d}t = f_i(x_j, t), \qquad i, j = 1, 2, 3, \ldots,$$

the explicit formula

$$x_i^1 = x_i^0 + \Delta t\, f_i(x_j^*, t^*), \tag{4}$$

where

$$t^* = t^0 + \tfrac{1}{2}\Delta t, \qquad x_i^* = x_i^0 + \tfrac{1}{2}\Delta t\, f_i(x_j^0, t^0),$$

and the superscripts 1 and 0 refer to the final point and the initial point respectively. In order that the formula (4) may be applied for the integration of equations (I16)–(I18), we require the values of the unknown quantities

$$\left(\frac{\partial u}{\partial r}\right)^*, \quad \left(\frac{\partial u}{\partial z} + \frac{\partial v}{\partial r}\right)^*, \qquad \text{and} \qquad \left(\frac{\partial v}{\partial z}\right)^* \tag{5}$$

correct to $O(\Delta t)$. For this, the bicharacteristics $\theta = \omega^* \pm \chi^*$ and ω^* through the intermediate point, say P^* (Fig. 1), are traced back to the initial region. The bicharacteristics are labelled 1, 2, and 3 respectively and variables at the points where they meet the plane $t = t_0 - \Delta t$ are denoted by the corresponding subscripts. The points (r_i, z_i), $i = 1, 2, 3$, are determined from

$$r_i = r^* - \tfrac{1}{2}\Delta t(u^* + A^* \cos \theta_i^*)\,, \qquad z_i = z^* - \tfrac{1}{2}\Delta t(v^* + A^* \sin \theta_i^*)\,,$$

correct to $O(\Delta t)$. The values of λ_i, ω_i, and all the physical variables can now be obtained at these points in the initial region.

In this paper we have approximated the point (r_3, z_3) with the point (r^0, z^0) itself. This accords with our limit of accuracy, as can be shown following Whitham (1958) and is, in fact, similar to his approximation of applying the compatibility relation along a characteristic to the flow quantities just behind the shock wave for two-variable problems. This simplifies the interpolations at the point (r_3, z_3) to a considerable extent. The distributions of λ and ω at the different points on the shock front at an initial time are expressed in terms of respective Chebyshev series, so that their values at any other point on the front as well as their derivatives along the front can be conveniently evaluated. The values of other flow variables can now be determined with the help of the shock relations (I9). Using these relations, the respective compatibility relations along the three bicharacteristics 1, 2, and 3 are

$$-\sin^2(\omega+\chi)\frac{\partial u}{\partial r} + \tfrac{1}{2}\sin 2(\omega+\chi)\left(\frac{\partial u}{\partial z} + \frac{\partial v}{\partial r}\right) - \cos^2(\omega+\chi)\frac{\partial v}{\partial z}$$

$$= \zeta_1 \frac{\mathrm{d}\lambda}{\mathrm{d}t} + \zeta_2 \sin\chi \frac{\mathrm{d}\omega}{\mathrm{d}t} + \zeta_3 \sin\chi + \zeta_4\,,$$

$$-\sin^2(\omega-\chi)\frac{\partial u}{\partial r} + \tfrac{1}{2}\sin 2(\omega-\chi)\left(\frac{\partial u}{\partial z} + \frac{\partial v}{\partial r}\right) - \cos^2(\omega-\chi)\frac{\partial v}{\partial z}$$

$$= \zeta_1 \frac{\mathrm{d}\lambda}{\mathrm{d}t} - \zeta_2 \sin\chi \frac{\mathrm{d}\omega}{\mathrm{d}t} - \zeta_3 \sin\chi + \zeta_4\,,$$

and

$$\sin^2\omega\frac{\partial u}{\partial r} + \tfrac{1}{2}\sin 2\omega\left(\frac{\partial u}{\partial z} + \frac{\partial v}{\partial r}\right) - \cos^2\omega\frac{\partial v}{\partial z}$$

$$= \zeta_5 \frac{\mathrm{d}\lambda}{\mathrm{d}t} + \zeta_6\,,$$

where

$$\zeta_1 = (3\lambda^2 - 3\lambda - E^{-1})EU^2/\lambda^3 A^2\,,$$

$$\zeta_2 = (\lambda-1)U/\lambda A\,,$$

$$\zeta_3 = (-\zeta_7 \sin\omega + \zeta_8 \cos\omega)\frac{\lambda-1}{\lambda \rho_0 A} - \frac{(\lambda-1)b_0^2 \sin\omega}{Ar}\,,$$

$$\zeta_4 = 3\left(\frac{\lambda-1}{\lambda^2}\right)\frac{U^3}{A^2}(\zeta_9 \cos\omega + \zeta_{10}\sin\omega) + \zeta_{16}\,,$$

$$\zeta_5 = \{(\lambda-1)(2U + A\lambda)E\lambda - U\}U/\lambda^3 A^2\,,$$

$$\zeta_6 = \left(\zeta_{12}\frac{\partial p_0}{\partial r}+\zeta_{13}\frac{\partial B_0}{\partial r}+\zeta_{14}\frac{\partial \rho_0}{\partial r}\right)\cos\omega$$

$$+\left(\zeta_{12}\frac{\partial p_0}{\partial z}+\zeta_{13}\frac{\partial B_0}{\partial z}+\zeta_{14}\frac{\partial \rho_0}{\partial z}\right)\sin\omega+\frac{(\lambda-1)b_0^2\cos\omega}{Ar}+\zeta_{15},$$

$$\zeta_7 = \left(\frac{6FU^2}{\lambda}-1\right)\frac{B_0}{\mu}\frac{\partial B_0}{\partial r}-(3Fb_0^2+3Hc_0^2-1)\frac{U^2}{\lambda}\frac{\partial \rho_0}{\partial r}+\left(\frac{3\gamma HU^2}{\lambda}-1\right)\frac{\partial p_0}{\partial r},$$

$$\zeta_8 = \left(\frac{6FU^2}{\lambda}-1\right)\frac{B_0}{\mu}\frac{\partial B_0}{\partial z}-(3Fb_0^2+3Hc_0^2-1)\frac{U^2}{\lambda}\frac{\partial \rho_0}{\partial z}+\left(\frac{3\gamma HU^2}{\lambda}-1\right)\frac{\partial p_0}{\partial z},$$

$$\zeta_9 = \frac{2B_0F}{\mu\rho_0}\frac{\partial B_0}{\partial r}-(Fb_0^2+Hc_0^2-\tfrac{1}{3})\frac{1}{\rho_0}\frac{\partial \rho_0}{\partial r}+\frac{\gamma H}{\rho_0}\frac{\partial p_0}{\partial r},$$

$$\zeta_{10} = \frac{2B_0F}{\mu\rho_0}\frac{\partial B_0}{\partial z}-(Fb_0^2+Hc_0^2-\tfrac{1}{3})\frac{1}{\rho_0}\frac{\partial \rho_0}{\partial z}+\frac{\gamma H}{\rho_0}\frac{\partial p_0}{\partial z},$$

$$\zeta_{11} = \{(\lambda-1)U+\lambda A\}/\rho_0\lambda^2A^2,$$

$$\zeta_{12} = \left(\gamma\frac{\lambda-1}{\lambda}(2U+\lambda A)HU+1\right)\zeta_{11}-\frac{1}{\rho_0 A},$$

$$\zeta_{13} = \left(2\frac{\lambda-1}{\lambda}(2U+\lambda A)FU+1\right)\zeta_{11}\frac{B_0}{\mu}-\frac{B_0}{\mu\rho_0 A},$$

$$\zeta_{14} = \left(U-(2U+\lambda A)(Fb_0^2+Hc_0^2)\right)\frac{\lambda-1}{\lambda}U\,\zeta_{11},$$

$$\zeta_{15} = \left(p_0+\frac{\lambda-1}{\lambda}U^2\rho_0+\tfrac{1}{2}(1-\lambda^2)b_0^2\rho_0\right)\frac{(\lambda-1)\gamma U\cos\omega}{\rho_0\lambda^2A^2r},$$

and

$$\zeta_{16} = \left\{p_0+\frac{\lambda-1}{\lambda}U^2\rho_0+\tfrac{1}{2}\left(1+\frac{2\lambda}{\gamma}-\lambda^2\right)b_0^2\rho_0\right\}\frac{(\lambda-1)\gamma U\cos\omega}{\rho_0\lambda^2A^2r}.$$

If these equations are applied in difference form along the respective bicharacteristics, they may be solved for the three terms (5) at any unknown point P^*.

The system of differential equations (I16)–(I18) can now be integrated using formula (4). The integrations were performed on the CDC 3200 computer of Monash University with a time step $\Delta t = 0\cdot 1$ and were carried nearly as far out as the surface. Only the case with $M_{s,i} = 5$ and $\beta^2 = 0\cdot 01$ was considered. For the sake of comparison, the method discussed in Part I (Section VI) for recording the results of integration at any instant was followed.

V. Results and Discussion

The results of the foregoing integration determine completely the position and orientation of the shock front at any time as well as the flow behind it as it propagates outwards with the initial value of the shock Mach number $M_{s,i} = 5$ in the toroidal magnetic field whose strength corresponds to $\beta^2 = 0\cdot 01$. The variations recorded for some of the shock parameters are presented in the following figures.

The corresponding curves obtained in Part I have also been depicted therein for the sake of comparison and they appear as dashed lines.

(i) *Density Ratio*

Figure 2 depicts the variations of λ_0 and λ_2 as functions of $\bar{R}_0$. The nature of these variations are similar to those obtained in Part I. We observe, further, that though the values of λ obtained in the present case never exceed those obtained in Part I, the difference itself is very small and is always less than $0 \cdot 5\%$. In fact, this difference can be seen to be negligible in the layers beyond $0 \cdot 6\,\bar{R}$.

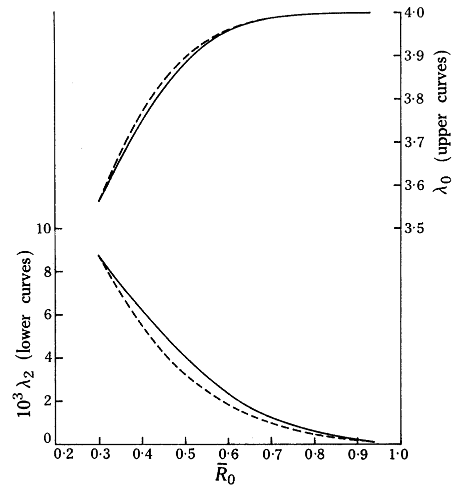

Fig. 2.—Profiles comparing the variations of density ratio λ in the present case (solid curves) with those obtained in Part I (dashed curves), as a function of $\bar{R}_0$.

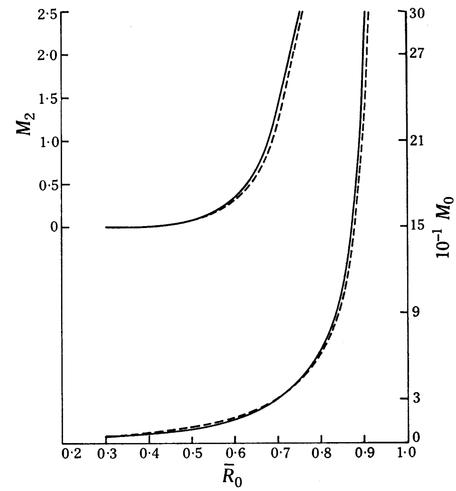

Fig. 3.—Profiles comparing the variations of shock Mach number M in the present case (solid curves) with those obtained in Part I (dashed curves), as a function of $\bar{R}_0$.

(ii) *Shock Mach Number*

The variations of M_0 and M_2 (Fig. 3), and hence of M itself, obtained in the present case are also similar to those obtained in Part I. Though the overall values of M in this case are smaller within the region $R = 0 \cdot 7\,\bar{R}$ and greater outside this region than the corresponding values in Part I, it is found that the difference does not exceed 10% anywhere inside the region $0 \cdot 85\,\bar{R}$. Beyond this region, the difference does grow large; nevertheless, as pointed out in Part I, results obtained for this region may not be physically relevant because of the neglect of radiative processes.

The variations of other parameters and physical variables are also in good agreement with those obtained in Part I, as can be expected after comparing respective values of λ and M, and bearing in mind that the values of the flow variables behind the shock can always be expressed in terms of two shock parameters and the values of the physical variables in the medium ahead of the shock front.

The results obtained in the present paper are correct to second order in Δt only, and in view of this the agreement of the results is very good. The inclusion of the terms involving spatial derivatives of velocity components gives rise to considerable complexity in integration, which may lead to large computational errors if we try to find results correct to higher orders in Δt. It is possible to minimize these errors; but this would involve much computational time. The results of this paper show that whilst it is possible to devise computational schemes to deal with equations of the type (I16), the simpler treatment given in Part I is sufficiently accurate to determine the essential features of the shock propagation.

VI. Acknowledgment

The author wishes to thank Dr. E. D. Fackerell for stimulating discussions and for a critical reading of the manuscript.

VII. References

Butler, D. S. (1960).—*Proc. R. Soc.* A **255**, 232.

Courant, R., and Hilbert, D. (1965).—"Methods of Mathematical Physics." Vol. 2, Ch. 6. (Interscience: New York.)

Whitham, G. B. (1958).—*J. Fluid Mech.* **4**, 337.